Overview of Harmonic and Resonance in Railway Electrification Systems

Haitao Hu , *Member, IEEE*, Yang Shao, Li Tang , Jin Ma , *Senior Member, IEEE*,
Zhengyou He , *Senior Member, IEEE*, and Shibin Gao

Abstract—Harmonic distortion and harmonic resonance problems have been widely concerned and reported in railway electrification systems (RESs) due to the harmonic injection from the nonlinear electric train, especially high-speed/high-capacity/large-power trains. This paper presents an overview of the harmonic and resonance problems in the RES, including harmonic problem composition, harmonic modeling, available influential factors assessment, harmonic resonance, and associated suppression methods. The harmonic problem mainly consists of the background harmonics brought from the utility system, resonance-region harmonics interacted by capacitive and inductive network elements, and characteristic harmonics generated from the switching process of the onboard power conversion system. The mathematical modeling and analysis methods are introduced, including frequency scanning analysis, S-domain analysis, resonance mode analysis, and modal sensitivity analysis. Available influential factors/parameters have been fully investigated against above-mentioned harmonic problems. Finally, different harmonic suppression methods have been compared and summarized in this paper.

Index Terms—Harmonic analysis, harmonic modeling, harmonic resonance, harmonic suppression, railway electrification system (RES).

I. INTRODUCTION

HARMONIC distortion has raised increasing attentions with the rapid development of the railway electrification system (RES), especially the high-speed railways (HSRs). The harmonic currents, generated from the thyristor- or pulse-width-modulation (PWM)-controlled converters in an electric train, flowing through the catenary network are one of the largest concerns. As a distributed *RLC* circuit, the catenary network can

Fig. 1. (a) Measured voltage and current waveforms under a resonance condition. (b) Measured catenary voltage harmonic distortions during a 24-h period (catenary-rail $V_{TR} = 27.5$ kV): (1) low-frequency background harmonics; (2) resonance-region harmonics; and (3) high-frequency characteristic harmonics.

experience series or parallel resonances at one or more specific frequencies that amplify harmonic currents. The measured voltage and current waveforms under a resonance are shown in Fig. 1(a). The highly distorted waveforms may lead to the electromagnetic interference in adjacent communication lines and the railway signaling system, overheating, and vibration at power capacitors, and maloperation at the protections. With the growing density of electric trains and increasing requests for power demand, harmonic pollution and resonance have become a major concern in both utility power system and RES.

A. Harmonic Problem Sources in RESs

Fig. 1(b) shows voltage harmonic contents obtained from the secondary-side voltage waveforms of a traction substation (TSS) during a 24-h period. Different harmonic sources are therefore, respectively, presented and generally cataloged as follows.

1) *Background voltage harmonics* are brought from aggravated harmonic injections of available nonlinear devices connected to the utility power system, and usually below 20 per unit (p.u.), i.e., 5-, 7-, 11-, 13-th harmonics [1], [2]. They can be measured in a new RES without train operations. Moreover, the background harmonics may be magnified by the series resonance.

2) *Harmonic resonance* is aroused through the interaction of capacitive and inductive elements/parameters, and excited by the current injection of the nonlinear train, which has been reported in many countries, such as South Korea [3], Italy [4], China [5], and Zimbabwe [6]. Two conditions required to stimulate a harmonic resonance are as follows.

    a) The system inductance and capacitance match with each other at some frequencies.

    b) A harmonic source, connected to the system, covers one or more of these resonance frequencies.

3) *Characteristic harmonics* generate inherently around the integer switching frequencies of the PWM-controlled 4-quardrant converter (4QC) of high-speed trains [7], [8]. As for the conventional electric train, the harmonics are characterized by rich low-frequency odd harmonics [9]. Apart from different harmonic spectra of different electric train types, they may have different harmonic behaviors by means of the equivalent output admittance.

B. Overview of Harmonic Studies in RES

Harmonic and resonance problems have been reported and investigated in many circumstances, such as low-voltage distribution systems and microgrids [10], [11], high-voltage transmission lines [12], substation and affiliated reactive-load compensation equipments [13], wind power systems [14], and electric railways [4]. The phenomena and impacts, harmonic modeling, series/parallel resonances, methodologies, mitigations for harmonic and resonance problems are under the intensive research interest.

Due to the specific circuit topology and nonlinear traction loads in RESs, this paper mainly concentrates on the overview of the harmonic and resonance problems in RESs. Many scholars in this field have put forward many analysis methods in recent decades. The influences of available factors, including primary/secondary supply lines, catenary lengths, traction transformer, interconnection point of rails, rolling stocks including trains' number, positions, and effort, have been investigated through simulations [15], [16].

In order to quantify the harmonic severity levels, some methods have been presented for studying the harmonic resonance. The methods can be roughly classified into the following four categories: frequency scan method [12], [17], [18], S-domain mode method [19], [20], harmonic magnification method [3], [6], and resonance mode assessment (RMA) or modal sensitivity indices [21], [22]. Different methods can obtain different noteworthy information, such as resonance frequencies, resonance amplitudes, critical resonance nodes, resonance locations, and their corresponding sensitivities.

Recent harmonic modeling methods for the RES are mainly based on either mathematical models or simulation models [3], [23]. Analyzing the former condition without considering the nonlinear load (NLL) model or modeling them as a set of ideal current harmonic sources are not rigorous. Several uncoupled or coupled NLL models are discussed in [24]–[26], such as Norton, crossed frequency admittance matrix, and frequency-coupled matrix approaches to describe the external features of NLLs for harmonic studies. The catenary network has a complex network structure, and the multitransmission lines (MTL) approach is adopted for modeling the catenary network. The completed model of the RES has been studied and discussed in [27].

The harmonic problem is influenced by different electrical parameters of the system, including the power system, the traction system, and the train control system. The structure or capacity of the power system will influence the background harmonics [28]. The parameters of the electric train's control system will change characteristic harmonics easily [8], [29]. Meanwhile, resonance and parameters of the RES are closely related, such as the length of the catenary network, impedance of the traction transformer, multiple railway lines, etc. [15]. Thus, different influential factors will affect harmonic and resonance behaviors in the RES.

The serious harmonic distortion will cause power quality problems, such as the motor failure, the arrester explosion, the potential transformer breakdown, etc. [30], [31]. Thus, available harmonic suppression methods are then considered to overcome the harmonic problems in the RES, such as optimizing the structure of the power system, installing power filters in the train or the TSS, and adjusting sensitive parameters of the traction system to change the resonant impedance amplitude and the frequency [22], [32], [33].

C. Contribution and Organization

As shown in Fig. 2, an overview schematic diagram of the harmonic and resonance in the RES is proposed. Based on our harmonic and resonance works in the RES, the fundamental contribution of this paper is to present an overview of different harmonic generation sources, harmonic modeling, available influential factors, analysis methods, and suppression schemes for the RES. Moreover, some new phenomena of harmonic and resonance from measured and simulation results have been discussed. Available influential factors are fully investigated, and resonance sensitivity studies dealing with harmonic mitigations are discussed.

The rest parts of this paper are organized as follows. The topology and harmonic problems of the RES are described in Section II. The completed harmonic modeling of each component is arranged in Section III. Different resonance analysis methods are summarized and further applied to analyze the harmonic resonance problems in Section IV. Available influential factors of the harmonic resonance are discussed in Section V. Section VI describes the harmonic penetration and assessment with different types of electric trains. Section VII summarizes and compares the suppression methods in dealing with three
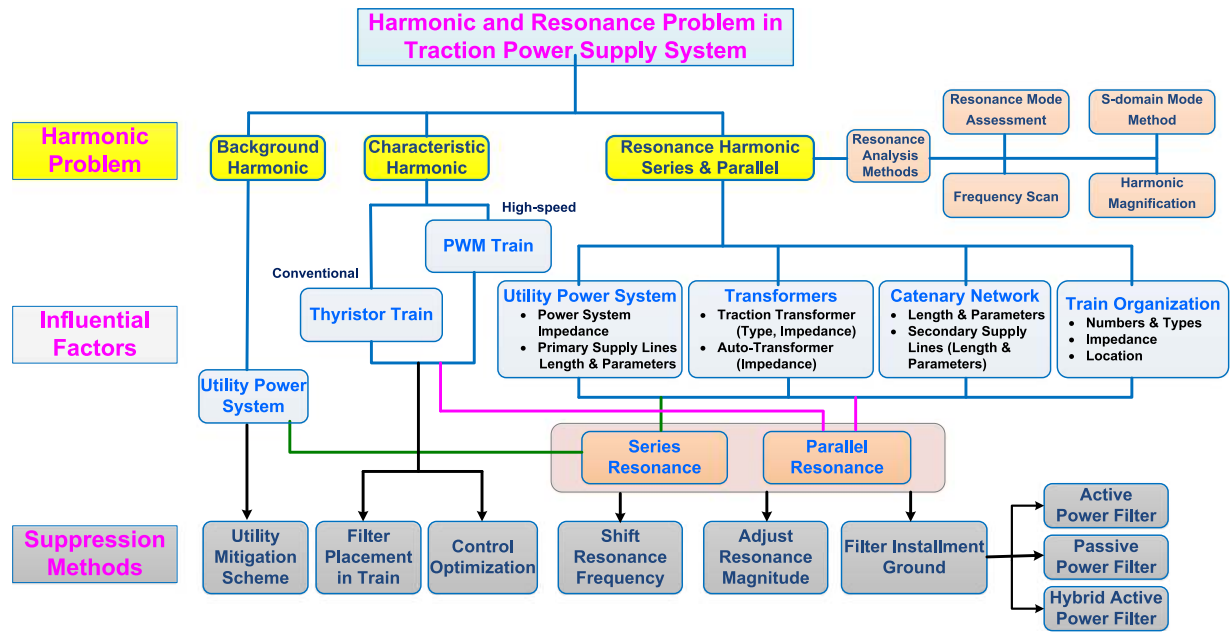
Fig. 2.   Overview schematic diagram of harmonic and resonance in the electric railway system.
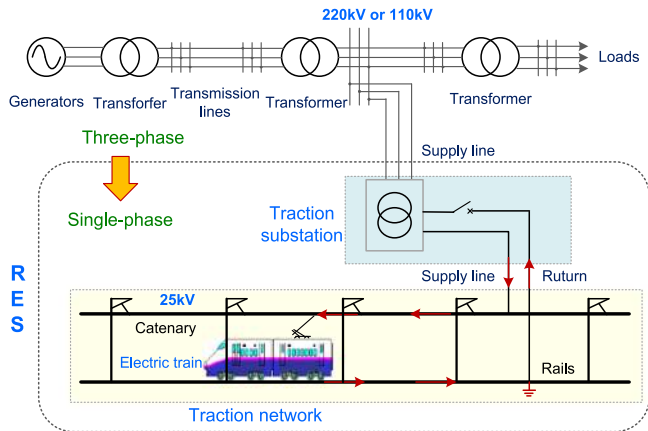

Fig. 3.   System topology of a typical RES.

Fig. 4.   95% maximum values of background harmonic voltages.

harmonic problem sources of the RES through simulation studies. Finally, a discussion and conclusion section are added in Section VIII.

II. DESCRIPTION OF THE RES AND ITS HARMONIC PROBLEMS

A. Typical RES Configuration

The ac RES, a specific single-phase power grid, is shown in Fig. 3. The system mainly consists of the TSS, catenary network, and electric trains. It normally takes the electricity from the three-phase upstream power grid (normally, 220/110 kV in China, 154 kV in South Korea, 225/400 kV in France, and 275 kV in Japan). Moreover, some countries, such as Germany and Norway, have their own dedicated power plants and distribution grids and their characteristics vary significantly. The voltages are stepped to two single-phase feeders via secondary supply lines to the catenary network. The electricity is finally supplied to the electric train through the contact of the pantograph–catenary system.

B. Background Harmonics

The background harmonics observed from the TSS are described as harmonic voltages that consist of the harmonics caused by available NLLs and power-electronics-based generations connected to the utility power system and the infiltration of the harmonic from associated TSSs on the operation railway. The background harmonics may be easily magnified when the series resonance exists in the traction system [34]. With the application of PWM technique in modern high-speed trains (HSTs), low-frequency harmonic contents are significantly reduced [31], [35] and are comparable to background harmonics so that the background harmonic in the HSR cannot be ignored.

The harmonic voltage spectra of the primary utility system could be obtained by the field data measured in the Skylight period of Hongqiao hub TSS without train operations in Shanghai, China. According to the continuous 24-h measured data, the 95% maximum values of three-phase background harmonic voltages are illustrated in Fig. 4, and one can find that the third, fifth, seventh, 11st, and 13rd harmonic voltages are high

Fig. 5. Harmonic current spectra of different trains. (a) Thyristor-controlled conventional train. (b) PWM-controlled high-speed train.

since the power system contain enough nonlinear loads such as three-phase bridge rectifiers whose characteristic harmonics are $6n \pm 1$ p.u. $(n = 1, 2, 3, \ldots)$.

C. Characteristic Harmonics of Electric Train

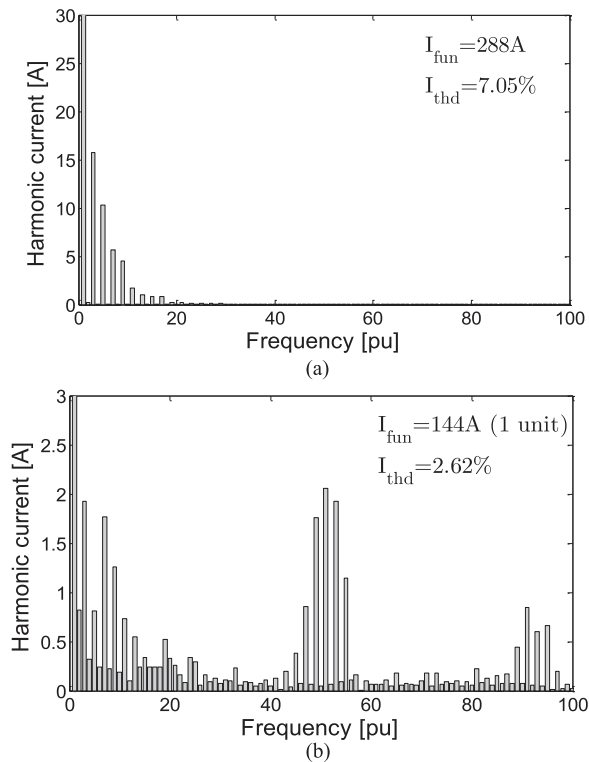The train is the main harmonic source in the RES, and its injected harmonic currents are found in abundance. The driving modes of electric trains are different and can be divided into two types, i.e., ac–dc type (thyristor-controlled conventional train) and ac–dc–ac type (PWM-controlled high-speed train). Thus, different current spectra generated by these trains are measured and compared in Fig. 5.

For a thyristor-controlled train [7], the measured current spectrum of the SS-type train (in China) is shown in Fig. 5(a), and the harmonic current values are listed in Appendix I. The harmonic current has rich content and concentrate at the low frequency region (third, fifth, seventh, etc.), and the high-frequency harmonic current contents are decreased with the increasing of frequency.

On the other hand, the high-speed trains controlled by the PWM-controlled 4QC share less harmonic issue concerns due to the adoption of high switching frequency PWM. In Fig. 5(b), the HST has reduced the lower order harmonics remarkably, but the high-frequency components, especially the characteristic harmonics near to the switching frequency, remain serious. The power factor of HST shows a relatively large increasement and almost close to 1 and the total harmonic distortion (THD) of the injected current is usually below 5%.
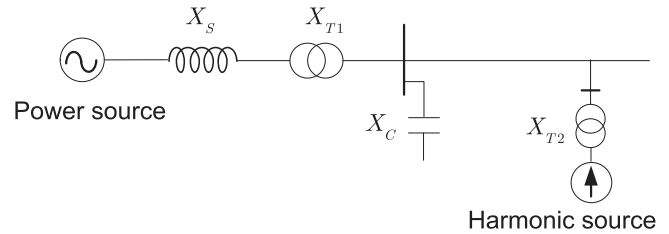

Fig. 6. Simple resonant circuit.

D. Resonance Harmonics

Harmonic resonance is the frequent reactive power exchange at the resonance frequency between the inductive and capacitive components in the RES. Resonances will amplify the injected harmonic current from the train through the catenary network lines. Generally, harmonic resonances can be categorized as series resonance and parallel resonance [36].

As shown in Fig. 6, viewed from the load side, the capacitor is in parallel with the harmonic source, the harmonic current coming from NLL may be near the parallel resonance frequency between the capacitance and the inductance of the overhead lines or transformers, then, the harmonic may be seriously magnified. Viewed from the grid side, background harmonics may be close to the series resonance frequency between the capacitors and grid inductance, then, the background harmonic in the power grid will be magnified.

Series resonance between the capacitance and grid inductance may magnify background harmonic current and worsen the harmonic current distortion point of common coupling. The series resonance problem in the RES was reported in [37] and [38] due to the connection of Steinmetz circuit which is used to correct unbalance voltages of the TSS. Resonance between the Steinmetz circuit and supply system reactances "observed" from the traction network is usually a series resonance.

III. HARMONIC MODELING FOR THE TRACTION SYSTEMS

A. Power System Model

A three-phase power system can be considered as a coupling circuit, and the coupled Norton model is adopted to represent such a system. Primary supply lines can be represented as a six-port MTL between the utility system and TSS [23].

B. MTL-based Catenary Network Model

1) Secondary Supply Line: The secondary supply lines connected from the TSS to the catenary network use power cables widely. The supply lines with nonnegligible distributed capacitances play an important role in resonance behaviors. Considering the transmission line theory, the supply line is usually modeled by an equivalent PI circuit, and its nodal admittance matrix is presented as the primary supply line.

2) Catenary Network: The MTL model is effective in representing the auto-transformer (AT)-fed catenary network [16]. Considering the relatively large leakage conductance of the return circuit to the ground, the multiport equivalent PI-type
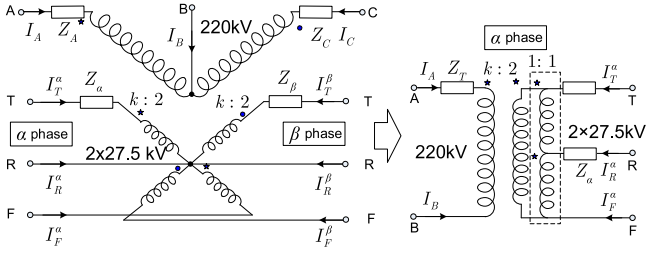
Fig. 7. V/x traction transformer model.

circuit model is used to represent each MTL segment. TSS, ATS, trains, section posts (SPs), and different area geography are the truncated slices in the MTL model, which "cut" the catenary network into several sections. The parameters of the PI-based MTL model are expressed as

$$Z_\pi = T_V \cdot \left[\frac{\sin(\gamma x)}{\gamma}\right] T_V^{-1} \cdot Z \tag{1}$$

$$Y_{\pi/2} = Z^{-1} T_V \left[\gamma \tan h\left(\gamma x/2\right)\right] T_V^{-1} \tag{2}$$

where x is the length of an MTL segment, $\frac{\partial^2}{\partial x^2} V_m = [\gamma^2]V_m$, $V_m = T_V^{-1}V_p$. V is the voltage vector of multiple conductors. γ is the eigenvalue matrix through phase-model transformation, $[\gamma^2] = T_V^{-1}[ZY]T_V = [\text{diag}(\gamma_1^2 \cdots \gamma_N^2)]$, Z and Y are the impedance matrix and admittance matrix of an MTL segment, respectively.

Multiple lines in the catenary network will lead to a nodal admittance matrix with huge dimensions. Therefore, this paper merged these lines into five equivalent conductors according to the electrical connection relationship. They are T buses (including a contact wire and a messenger wire) in up and down tracks, F buses (including a positive feeder) in up and down tracks, and R bus (including four rails, two protection wires, and 2 integrated earth wires).

C. Transformer Model

Transformers are considered by its low-frequency equivalent model, which adds capacitances that allow to take into account the displacement currents inside the equipment at higher frequencies. Here, we are not considering the capacitance of transformers for simplifying the analysis.

1) Traction Transformer: There are many different connections of traction transformers, such as single-phase, Ynd11, V/v(V/x), and Scott [39]. The V/x traction transformer is widely used in Germany and China HSR due to its high capacity utilization, simple wiring, and easy interface to AT catenary network. The V/x transformer contains two single-phase three-winding transformers, which supply power for both sides of the feeding section. The two windings, whose voltages are ±27.5 kV due to the extracted and grounded neutral point of the secondary winding, are connected to the T bus and F bus. Fig. 7 shows the equivalent circuit of the V/x transformer and its alpha phase.

The nodal admittance matrix of the V/x transformer can be described by

$$\begin{bmatrix} I_P \\ I_S \end{bmatrix} = \begin{bmatrix} Y_{PP} & Y_{PS} \\ Y_{PS}^T & Y_{SS} \end{bmatrix} \begin{bmatrix} V_P \\ V_S \end{bmatrix} = Y_T \begin{bmatrix} V_P \\ V_S \end{bmatrix}. \tag{3}$$

The vectors in (3) are listed as follows:

$$\begin{cases} I_P = \begin{bmatrix} I_A & I_B & I_C \end{bmatrix}^T \\ V_P = \begin{bmatrix} V_A & V_B & V_C \end{bmatrix}^T \\ I_S = \begin{bmatrix} I_T^\alpha & I_F^\alpha & I_R^{\alpha\beta} & I_T^\beta & I_F^\beta \end{bmatrix}^T \\ V_S = \begin{bmatrix} V_T^\alpha & V_F^\alpha & V_R^{\alpha\beta} & V_T^\beta & V_F^\beta \end{bmatrix}^T \end{cases} \tag{4}$$

The modeling method of other traction transformers is similar according to the mathematical model theory, and another detailed traction transformer model is shown in Appendix II.

2) Auto-Transformer: AT is concatenated to the contact line and positive feeder, and its extracted neutral point is connected to rails or directly grounded. The up-track and down-track, shorted out by an extremely small resistance ε, respectively, will power for the same AT in the all-parallel AT traction network. The modeling approach has been worked out in [40].

D. Harmonic Modeling for the Electric Train

Harmonic modeling for the electric trains, especially the 4QC controlled by the PWM technique, dominates the resonance behaviors of the traction drive system. There are available modeling methods to represent the harmonic current of the train, such as in [3] and [16] adopting a set 1 p.u. harmonic currents. An ideal current source can inject specific harmonics for testing the harmonic impedance behaviors observed from the train (or pantograph). But this method can only test the traction network resonance not the whole RES. The 4QC of the trains are usually two level, multiple interlaced two-level or three-level converters, as shown in Fig. 8.

The ac-side voltage is determined from the switching functions and dc voltage in Fig. 8(c), thus, the input current is obtained as

$$I_S = \frac{V_S(1) - V_{\text{ac}}(1)}{R_S + j\omega_0 L_S} - \sum_{h=2}^{H} \frac{V_{\text{ac}}(h)}{R_S + jh\omega_0 L_S} \tag{5}$$

V_{ac} and V_S are the primary- and secondary-side voltages of the converter, respectively. R_S and L_S are the equivalent resistance and inductance of the traction transformer, respectively, and 1 and h are the fundamental and harmonic orders, respectively.

If the 4QC of the train is two level, the signal is S_A (same to S_B with 180° shifting) and the three-level or two-interlaced signal is S_{AB}. Associated harmonic spectra of S_A and S_{AB} are presented in Fig. 9. As described in [21] and also from the measurements of Chinese electric trains, the dominant harmonics all center around 4× switching frequency for three-level PWM converter, 2× switching frequency for two-level PWM converter, and 2 n× switching frequency for n-interleaved two-level PWM converter.

Fig. 8.   Schematic diagram of a drive unit of CRH380A. (a) Two-level 4QC. (b) Interlaces two-level 4QC. (c) Three-level PWM converter.

Fig. 9.   Fourier results of injected current, the THDs are 12.96% and 3.29%, respectively.

1) Constant Current Harmonic and Measured-Based Model: The harmonic current model is usually used to model the train. The model will be so effective that the complex internal structure of NLLs is simplified, and the harmonic current characteristics are used to study the harmonic problems of the system. The probability distributions of the train harmonic currents are obtained by the measured data. The constant harmonic source model will correctly represent the harmonic behaviors of the electric train.

Fig. 10.   Harmonic current of different cases measured from a three-level 4QC.

Harmonic currents, measured from a power unit of China HST, in different cases are presented in Fig. 10. Six sets of current parameters are represented to cover multiple operation modes of the HSTs. The operation modes are, namely, tractive full-load, tractive middle-load, tractive small-load, braking small-load, braking middle-load, and braking full-load. The harmonic current concentrated within 20 p.u. when the train operation mode is tractive full-load. The harmonic current of tractive middle-load and tractive small-load are similarly concentrated at low orders and around 30 to 50 p.u., respectively. The power of the barking regeneration mode is less than that of the traction modes, and its harmonic current content is less than the traction mode. When the train operates in the barking middle-load condition, the low-frequency harmonic currents are rich. The harmonic currents of barking full-load are well distributed, and individual order is high, e.g., 25 p.u., 39 p.u., 51 p.u., etc. The harmonic current distribution is different when the train operating under six conditions. Therefore, constant harmonic source models of different conditions are considered by the measured data [1], [23].

2) Norton Model: The drive unit of the HST is a typical nonlinear device, which consists of the onboard traction transformer, 4QC, dc-link, inverter, and motors. The Norton model is utilized to represent the NLL of train's harmonic studies [24]. The Norton equivalent harmonic model and the injected harmonic currents of a train can be obtained as

$$
\begin{bmatrix} I_s(1) \\ I_s(2) \\ \vdots \\ I_s(n) \end{bmatrix} = \begin{bmatrix} y_s(1) & 0 & 0 & 0 \\ 0 & y_s(2) & 0 & 0 \\ 0 & 0 & \ddots & 0 \\ 0 & 0 & 0 & y_s(n) \end{bmatrix} \times \begin{bmatrix} V_s(1) \\ V_s(2) \\ \vdots \\ V_s(n) \end{bmatrix}
$$
$$
- \begin{bmatrix} y_s(1)V_{ac}(1) \\ y_s(2)V_{ac}(2) \\ \vdots \\ y_s(n)V_{ac}(n) \end{bmatrix} \tag{6}
$$

where $y_s(k)$, $V_s(k)$ are the kth harmonic equivalent admittance and harmonic voltage on the secondary side of the traction
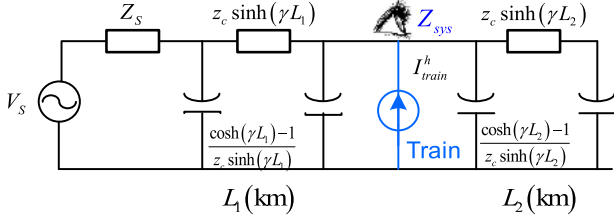
Fig. 11. Harmonic transmission model of T-type catenary circuit.

transformer, respectively, and $V_{ac}(k)$ is the kth harmonic voltage of the grid side of the train.

3) Analytical Model: The drive unit of the HST is controlled by the three-level PWM converter, and an analytical solution for converter harmonics based on the double Fourier series theory is applied to model the train. The interlaced two-level PWM converter is presented in Fig. 8. Assume that the ac-side voltage is sinusoidal, the dc-link voltage is constant, and the switching operation is ideal. Based on the double Fourier series method, the input voltage V_{31} of the interlaced three-level PWM converters with enhanced sampling scheme given in Fig. 8 is shown as [8], [15], [41]–[43]

$$V_{31}(t) = \sum_{h=1,3,5,\ldots}^{\infty} \frac{8 J_n \left(\frac{np\varepsilon M\pi}{2} \right)}{np\varepsilon\pi} \sin \left(n\omega_m t - \frac{np\varepsilon\pi}{2} \right)$$

$$+ \sum_{m=2,4,6,\ldots}^{\infty} \sum_{n=1,3,5,\ldots}^{\pm\infty} 8C_{mn} (-1)^{m/2} \sin$$

$$\times \left((m\omega_c + n\omega_m) t - \left(m\pi + \frac{np\varepsilon\pi}{2} \right) \right) \quad (7)$$

where $C_{mn} = \frac{J_n \left[(m + n\varepsilon p) \frac{M\pi}{2} \right]}{\pi (m + n\varepsilon p)}$, $J_n(x) = \frac{(-1)^n}{2\pi} \int_0^{2\pi} e^{jx \sin y}$ $e^{jny} dy$ is n-order Bessel function, M is the modulate ratio, $p = \omega_m / \omega_c$, ω_c is the carrier angular frequency, ω_m is the modulation angular frequency, and ε is the sampling factor. Based on the assumption, the 4QC is therefore a voltage harmonic source. With the leakage impedance of the onboard transformer, it can also be seen as a Norton or Thevenin equivalent circuit.

The Norton model or the current source model is usually used to represent the harmonic behaviors of electric trains. Due to the time-varying operations of the train, the variation of the Norton model should be considered. A solution was made with considering different power demands in earlier and the admittance part can be found in [1].

IV. ANALYSIS METHODS

A. Harmonic Resonance Mechanism and Analysis Methods

The main mechanism of the harmonic resonance to detect the resonance point is searching the maximum magnification of the harmonic current. According to the steady-state equation and the equivalent circuit, neglecting the long-line effect, the parameters in Fig. 11 can be described as [3], [5]

$$Z_{\text{sys}} = \frac{Z_0 \cosh(\gamma L_2) \left[Z_S \sinh(\gamma L_1) + Z_0 \cosh(\gamma L_1) \right]}{Z_S \sinh(\gamma L) + Z_0 \cosh(\gamma L)} \quad (8)$$

where $\gamma = \sqrt{zy}$ is the propagation constant of the contact line. Catenary $Z_0 = \sqrt{z/y}$ is the characteristic impedance of the contact line. $L = L_1 + L_2$ is the length of the catenary line and L_1, L_2 are the left-side length and right-side length seen from the harmonic source, respectively.

In (8), the parallel resonance condition is $Z_S \sinh \gamma L + Z_0 \cosh \gamma L = 0$, which can be simplified as $Z_S = -Z_0/(\gamma L)$ due to $\gamma L \leq 1$ and $\tanh \gamma L \approx \gamma L$. If Z_S could be expressed by $Z_S = j\omega L_S$, the parallel resonant frequency will be $f \approx \frac{1}{2\pi \sqrt{L \times L_S c_{\text{pu}}}}$. Therefore, the resonance is highly dependent on the system impedance (grid, transformer, catenary), catenary length, and its per unit distributed capacitance.

To address the harmonic resonance problem, there are many methods presented for investigating resonance frequencies, amplifications, and sensitivity indices, such as RMA and its sensitive methods, S-domain modal method, and transfer function method. The common methods for the harmonic resonance analysis in the electric railways are mainly studied by measurements [4], time-domain simulations [5]–[7], and the frequency scan method [8]. These methods are widely adopted to investigate all parallel and series resonance frequencies in a linear network in frequency domain. Unfortunately, these tools cannot offer additional information, such as the importance of different buses or components in the network to the critical resonance, which is effective to solve the harmonic problems [10].

1) *Frequency scan method* was widely adopted in studying the harmonic resonance, and is also one of the most accurate and reliable analysis method [12]. It aims at obtaining the curves of different nodes whose driving impedance changes with the frequency. A peak value point in this curve represents a parallel resonance point, while a valley value in this curve represents a series resonance point. Frequency scanning method utilizes the system nodal voltage and injected current equation, i.e., $V_f = Y_f^{-1} I_f = Z_f I_f$. Each element z_{ij} in Z_f in the harmonic domain can represent the driving impedance seen from node i injected from node j.

2) *Resonance mode assessment method* offers additional information needed to solve the resonance problem. Harmonic resonance of a linear electrical system is associated with the nodal admittance matrix Y_f at frequency f. It can be decomposed as [15], [21]

$$Y_f = L\Lambda T \quad (9)$$

where L, $T(L = T^{-1})$ are the left and right eigenvector matrices, respectively. $\Lambda = \text{diag}(\lambda_1, \lambda_2, \ldots, \lambda_k, \ldots)$ is the diagonal eigenvalue matrix of Y. $1/\lambda_k$ can reflect the modal impedance of the linear electrical system.

The sensitivities of eigenvalue m with respect to Y_{ij} is defined as

$$S_{m,ij} = \frac{\partial \lambda_m}{\partial Y_{ij}} = t_{mi} l_{jm} \quad (10)$$

where Y_{ij} is the ith row and jth column entry of Y_f. The term $S_{m,ij}$ represents the bus sensitivity to a mode resonance or bus participator factor only when $i = j$.

TABLE I
ELECTRICAL PARAMETERS IN FIG. 11

$Zs = 0.562 + j8.073\,\Omega$	$L_1 = 15$ km	$L_2 = 10$ km	$Z_0 = 0.04 + j0.295\,\Omega/\text{km}$	$C_0 = 32$ nF/km

TABLE II
TYPICAL IMPEDANCE RATIO OF THE TRACTION SYSTEM

	Impedance/Ω	Utility	Transformer	Catenary
Conventional railway	$j22.042$	13.7%	22.9%	63.4%
High-speed railway	$j10.625$	1.5%	47.5%	51.0%

According to mathematical calculation, the modal impedance sensitivity and modal frequency sensitivity can be defined as the derivative of the modal impedance and frequency with respect to component parameter α [22], i.e., $dz_m/d\alpha$ and $df_m/d\alpha$. They can reflect the impacts of component parameters on the modal resonance impedance and frequency, and help us find the most sensitive component.

3) *S-domain mode method* is a kind of resonance analysis methods which transfers the nodal admittance matrix from frequency domain to s-domain [19]. Zeros and poles, which are the premise of determining series or parallel resonance, can be calculated by the transfer function between the nodal voltage and the injected current, utilizing the Newton iteration method.

The injected current $i_m(s)$ at bus m and output voltage $u_n(s)$ at bus n can be obtained as

$$G(s) = \frac{u_n(s)}{i_m(s)} = \boldsymbol{c}^T \cdot \boldsymbol{Y}(s)^{-1} \boldsymbol{b}. \tag{11}$$

In which, $\boldsymbol{b} = \begin{bmatrix} 0 & \cdots & 1_m & \cdots & 0 \end{bmatrix}^T$ is the injected current vector, $\boldsymbol{c} = \begin{bmatrix} 0 & \cdots & 1_n & \cdots & 0 \end{bmatrix}^T$ represents the investigated bus n. And the Newton iteration method can be used to calculate zeros and poles in identifying the series or parallel resonance, respectively.

The S-domain mode method has a faster calculation speed when compared to the frequency scanning analysis method. However, this method is somewhat sensitive to the initial value during the iterative process. Therefore, a proper initial value can improve the calculation speed and the convergence direction effectively.

B. Case Study for Harmonic Resonance

The electrical parameters are given in Table I, based on which the methods and the influential factors are compared. As listed in Table II, the impedance proportion of each components in the traction system also represents the influential degrees on the corresponding harmonic resonance.

The resonance results calculated through the frequency scan, RMA, and S-domain mode methods are presented in Fig. 12. As seen in Fig. 12(a), the frequency scan approach not only calculates the parallel resonance points of the peaks, but also determines the series resonance results of the valleys. The series resonance results are 29.81 p.u., 38.83 p.u., and 57.68 p.u. which
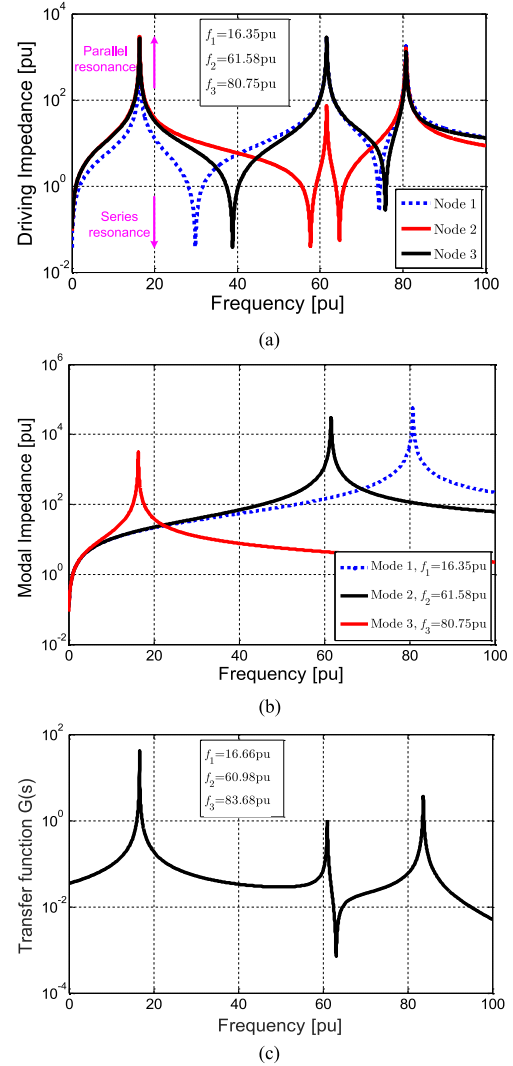

Fig. 12.   Resonance results. (a) Frequency scan. (b) Resonance mode assessment. (c) S-domain mode method.

are far from the scope of the background harmonics. In other word, this series is out of concern since that its frequencies mismatched with the background harmonics.

On the other hand, all the three methods can provide three parallel resonances, i.e., 16.35 p.u., 61.58 p.u., and 80.75 p.u. One can find that they could support similar parallel resonances. Each node of the frequency scan has all three resonances but the RMA only shows three modes representing independent resonance information. Additionally, the frequency scan curves are of redundancy and cannot support more effective information in making a mitigation scheme since all "resonance peaks and valleys" are seen equally important. Therefore, the RMA method and derived resonance sensitivity are applied in investigating the harmonic resonance behaviors of the RES.
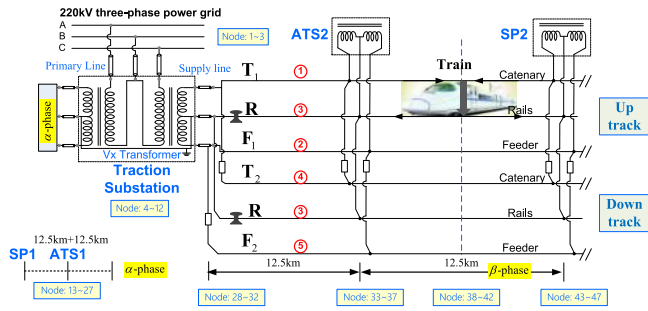
Fig. 13.   Typical HSR line with all-parallel AT catenary network.

The disadvantages of the S-domain mode method are as follows.

1) Complicated modeling and it is not possible to directly model the distributed components in S-domain.
2) It is so sensitive to the initial values that starting from a nonsuitable initial value cannot obtain the poles.
3) The amount of the iterative number and the calculation time may increase as the increasing nodes of the system. However, it may save time since they just need an iteration rather than a frequency scan process.

V. INFLUENTIAL FACTORS OF RESONANCE

A. System Configuration

A typical RES [44], [45] has been taken as an example of more complicated topology and electric elements. The RES, under case studies depicted in Fig. 13, consists of a traction transformer, primary/secondary supply lines, 2×25 kV AT catenary network, and integrated grounding lines. The case study system is a typical traction power system of an HSR in China [40], [46], South Korea [3], and Italy [16], [47]. The similar topology can be found in [48] and [49].

The three-phase 220 kV utility is stepped down to 2×27.5 kV by a V/x transformer in a TSS. The primary supply line connects upstream power substation and the TSS. Practically, a TSS offers multiple feeders for the up track and down track of one railway line or multiple railway lines (which is known as the hub TSS). The TSS is distributed about 40–60 km along the rail route, while the ATs installed in the AT substation (ATS) or SP are distributed about 10–15 km. The nodes are also numbered in Fig. 13. Detailed electrical parameters are selected from a Chinese electric railway for a study case, as listed in Appendix III.

B. Series Resonance

Fig. 14 gives the series results of one-line and five-line traction system. Series resonance points of each curve, seen from different network buses, are different. The dominant series resonance at 16.52 p.u. observed from the 220 kV utility grid should be considered. Moreover, the series resonance frequencies will be shifted toward the lower frequencies with the increasing of the supply lines, such as 7.61 p.u. with five supply lines. As a result, the background harmonic voltages may be amplified by the series resonance at the primary side of the TSS.
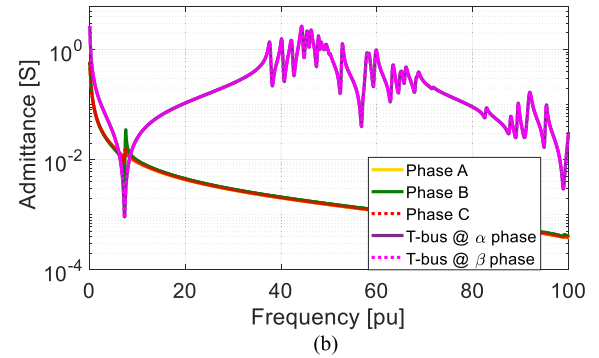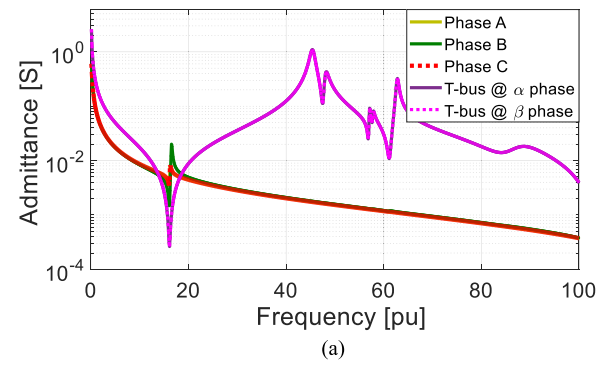

Fig. 14.   Series resonances seen from the utility power system. (a) One-line traction system. (b) Five-line traction system.
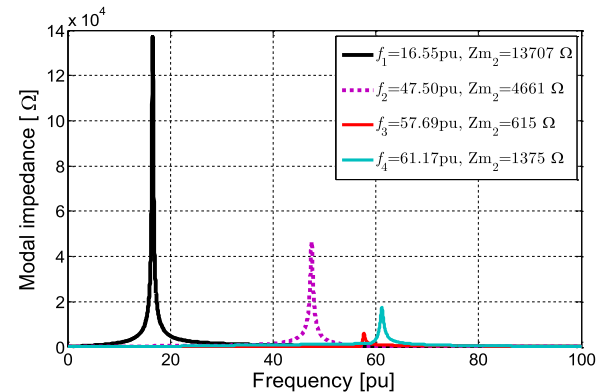

Fig. 15.   Resonance results obtained by the RMA method.

On the other hand, series resonances seen from 27.5 kV buses, far away from the frequency range of the background harmonics, are out of concern. Moreover, one can find that the admittances are slightly amplified at these series resonance frequencies. Therefore, majority of the resonance studies focuses on the parallel resonance due to the practical circuit topology and their parameters.

C. Parallel Resonance and Sensitivity Results

Fig. 15 shows the resonance results obtained from the RMA approach. The parallel resonances of the test system are 16.55 p.u., 47.50 p.u., 57.69 p.u., and 61.17 p.u., four different resonances.

As a result, derivating from the RMA method, the participation factor of each node and resonance sensitivity indices,
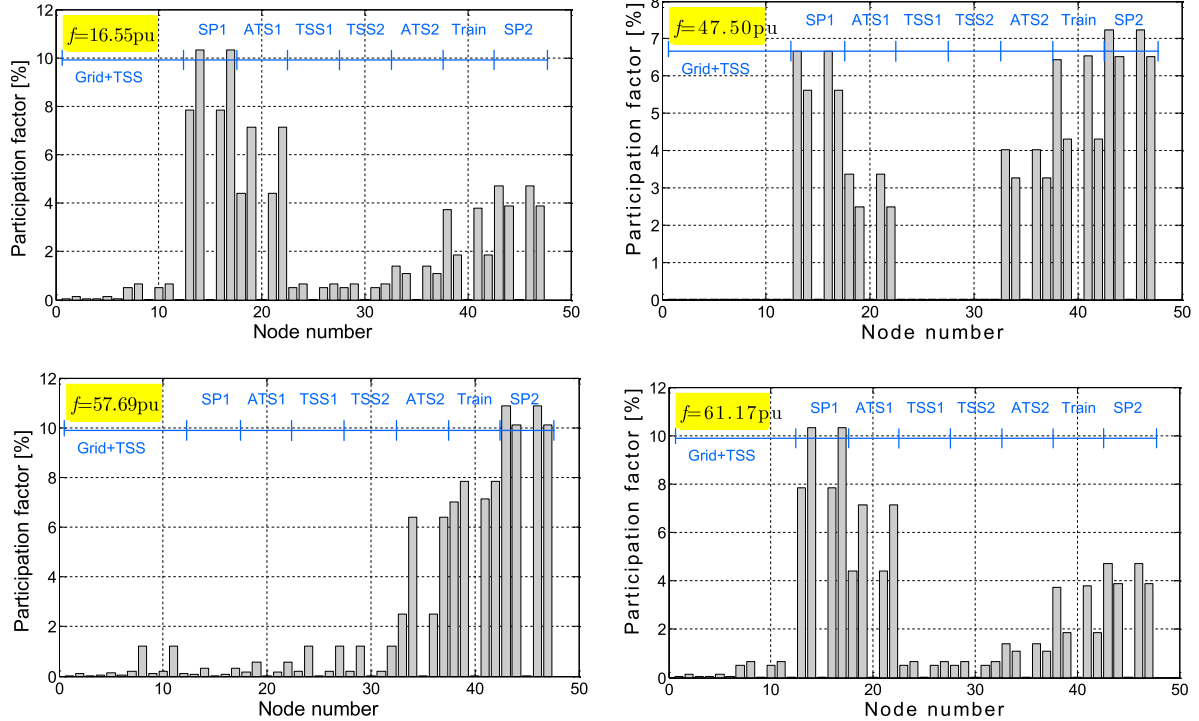
Fig. 16.   Participation factors of all nodes with respect to four resonance modes.

TABLE III
RESONANCE SENSITIVITY INFORMATION

Indices	C/L	RFS [Hz/%]	RIS [%/%]
System impedance	L	−30	5.13
Supply-line length	L	0	0
Secondary-line length	C	−10	−5.26
Secondary-line capacitance	C	−10	−4.37
Secondary-line inductance	L	0	7.37
Traction transformer impedance	L	−335	+27.73
Catenary line length	C	−440	−60.02
Catenary line Capacitance	C	−400	−76.43
Catenary line Inductance	L	−35	−3.53
AT impedance	L	−5	3.70
Train position	−	0	−3.90
Train impedance	L	−20	−5.51

including resonance frequency sensitive (RFS) and an resonance impedance sensitivity (RIS), of each parameter is applied here, as shown in Fig. 16. Note that the participation factors of the contact lines (or positive feeders) on up and down tracks are the same as they are directly connected at ATs in the all-parallel AT-fed catenary network. The contacts and positive feeders at the SP show the larger participation of the resonances, which can be selected to place a filter for mitigating the harmonic resonance. The rails, power system, and primary lines own ignored participations in resonances.

In order to clarify the impact of electrical parameters and components, the resonance sensitivity indices are applied here. Select $f = 16.55$ p.u. mode as an example. The resonance sensitivity indices are presented in Table III. Following interesting summarizations can be drawn.

1) The RFS indices are almost negative which shows that increasing the electric parameters corresponding to either L or C may decrease the resonance frequencies. It can be explained through Fig. 11 where the resonance frequency is $1/\sqrt{L_S C}$.
2) The network components are corresponding to the inductive or capacitive parameters. Therefore, increasing inductive components may decrease resonance magnitudes. Otherwise, increasing capacitive parameter increases resonance magnitude.
3) Electrical parameters of the catenary network and traction transformer dominate the primary resonance frequency and magnitude.

D. Simulations Results of Available Influential Factors

Some electrical parameters are so small that variations of them cannot show enough sensitivity. For example, the secondary line is only 150 m, and there are multiple lines in a hub TSS. Therefore, this section simulates and investigates the impact of these parameters.

1) Impact of Multiple Railway Lines on Resonances: Resonance results with multiple railway lines are shown in Fig. 17. The results include four scenarios, i.e., one line, two lines, five lines, and ten lines in a TSS, illustrate that the number of resonance points increase with the increase of railway lines. The conventional traction system with only one railway line has three dominant independent resonances. With the increasing number of railway lines, the number of resonances are becoming 11, 20, 49, respectively, and center in a frequency band. Just like "earthquake band," these bands are defined as
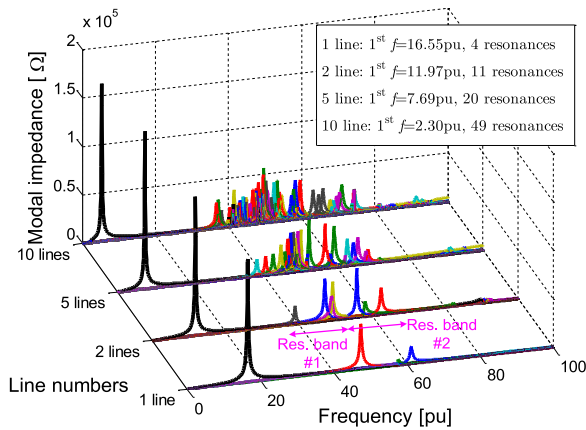
Fig. 17.   Resonance characteristic of different railway lines in a TSS.

"resonance bands." Meanwhile, the first resonance mode, separated from other resonances, is kept and shifted to the lower frequency.

In order to distinguish different resonance behaviors, therefore, the resonances are classified into two categories, i.e., primary resonance and resonance bands. In this case, the primary resonance has only one isolate resonance, and the resonance band owns multiple resonances gathering in a frequency low frequency. If the number of railway lines increases, the resonance band will be wider [15].

2) Impact of Train Organization (Positions, Numbers): The electric train is usually represented as two models in the harmonic domain, i.e., a harmonic current source and a Norton circuit. The resonance will not be affected if the train is equivalent to a harmonic current source. As for the Norton circuit model, the onboard transformer in the train has an equivalent impedance, which will change the system nodal admittance matrix and influence the results of resonance analysis.

The resonant results of different numbers of trains are shown in Fig. 18. Resonance frequencies increase when the number of train increases from 1 to 6. As early concluded in Section V-C, the energization of a train is equal to decrease the impedance from infinite to the equivalent impedance of the train. As a result, the primary resonance frequency would be increased and the amplitude would be decreased. However, it shows a slight influence on the resonance in terms of the number of trains.

Comparing Fig. 19(a) and (b), one can find that positions of a train have a slight impact on the primary resonance frequency. However, the number of the trains will affect the resonance frequency with about 100 Hz (2 p.u.) variation. Moreover, variations of the position and number of the trains have larger impact on $f = 47.50$ p.u. resonance. The impact of the position and number on this resonance frequency are within 1 p.u. and 4 p.u., respectively.

3) Impact of the Secondary Supply Line: The supply line is an important component in RES, and it mainly consists of the power cable with considerable capacitance. As the default length is only 0.15 km, the sensitivity values are relatively small. Therefore, in order to clarify the impact of the secondary sup-
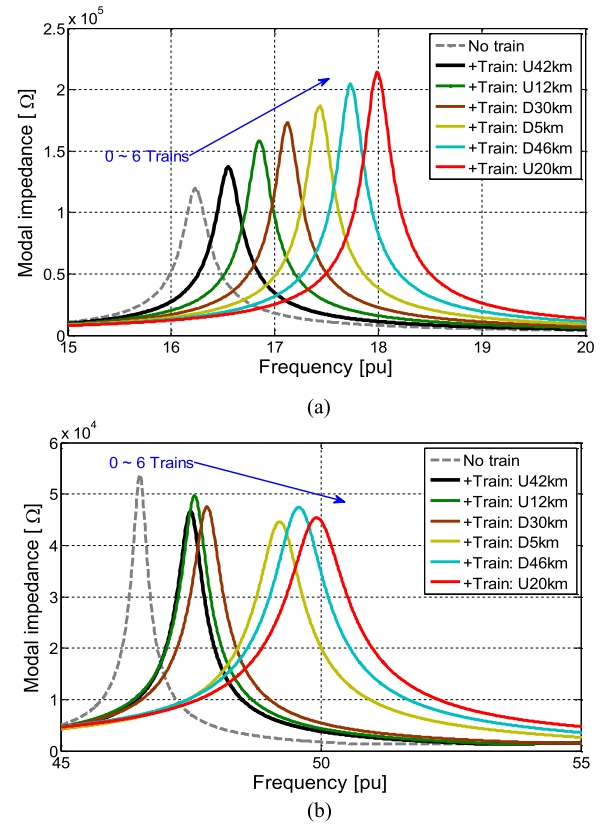

(a)

(b)

Fig. 18.   Impact of train number on resonance results: (a) $f = 16.55$ p.u. and (b) $f = 47.50$ p.u. "U" and "D" represent up and down tracks, respectively.

ply lines, the length is selected as 0∼5 km and corresponding resonance results are illustrated in Fig. 20. The resonance frequency is decreased about 250 Hz (5 p.u.) when increasing 5 km power cable, and the resonance amplitude is also decreased. The results make a good agreement with the obtained sensitivity indices given in Table III.

E. Summary

As discussed above, one can quantify impact levels of different electrical parameters with respect to resonance frequencies and amplitudes. The increase of all the inductive or capacitive equivalent parameters may decrease the primary resonance frequency.

1) Among electrical parameters, some of them have a strong influence on resonances, such as the traction transformer, catenary network, while others have a slight impact on resonances, such as the AT, primary/secondary supply line, and origination of the electric trains.

2) In other words, the sensitive parameters and corresponding devices can be effective in reducing harmonic and resonance problems. Fortunately, the sensitive information can be effective in designing an RES dealing with the harmonic and resonance problems.

3) Additionally, multiple railway lines increase the resonance points and result in the resonance band in a fre-
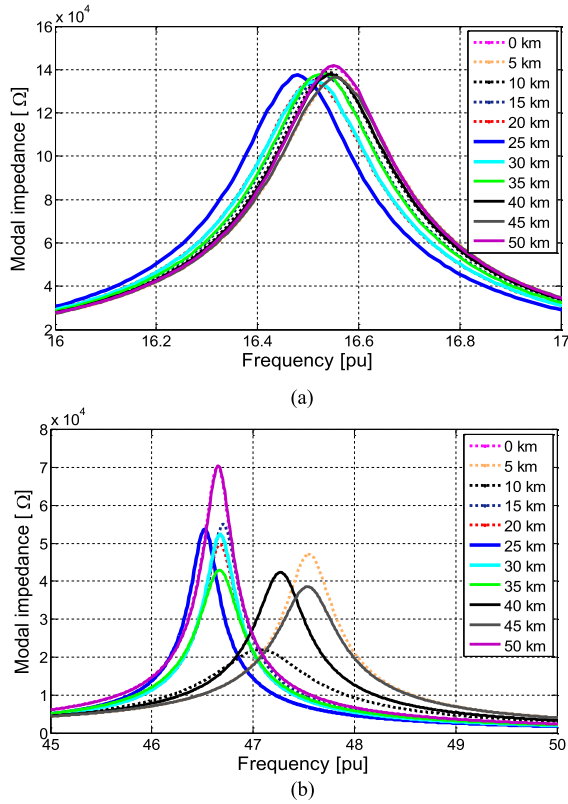
Fig. 19.   Impact of trains' positions on resonance results: (a) $f = 16.55$ p.u. and (b) $f = 47.50$ p.u.
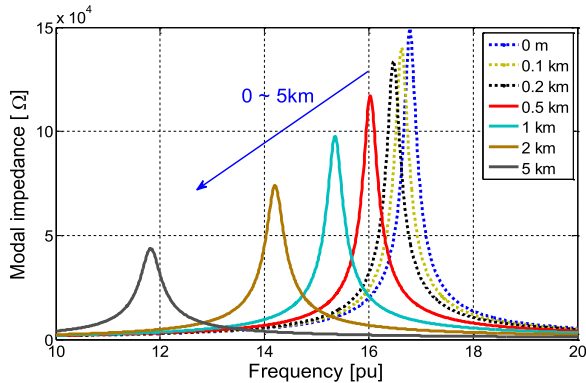

Fig. 20.   Impact of secondary supply lines on resonance results.

quency region. The resonance band allows us to treat them as a special resonance when a mitigation scheme is issued, since the individual suppression for each resonance point is not practical.

VI. HARMONIC PENETRATION AND ASSESSMENT

A. Fundamentals

Harmonic resonance is an important part of harmonic problems as well as characteristic and background harmonics mentioned earlier. Therefore, as mentioned in Section I, the harmonic distortion should be simulated with the impact of harmonic sources in the RES, such as background harmonics and

TABLE IV
BACKGROUND HARMONICS BETWEEN T-BUS AND RAILS AT THE TSS

h	Voltages/V	Phase/deg	h	Voltages/V	Phase/deg
3	109.61	62.9	11	77.76	113.5
5	159.44	250.0	13	67.16	164.4
7	135.06	294.5	15	8.72	132.5
9	22.17	0.20	17	21.60	244.3
			19	8.47	269.6

harmonic injection of different trains. Fortunately, the harmonic penetration dealing with harmonic power flow in this case is noniterative. Therefore, the hth harmonic flow can be solved through

$$\boldsymbol{V}_h = \boldsymbol{Y}_h{}^{-1}\boldsymbol{I}_h \tag{12}$$

where $\boldsymbol{I}_h$ is the harmonic injection vector; $\boldsymbol{Y}_h$ is the network nodal admittance matrix; and $\boldsymbol{V}_h$ is the voltage response vector.

Consequently, the conventional trains are represented by the current source model and PWM-based high-speed trains are represented by the Norton model that consists of the equivalent output admittance and injected harmonic currents. The measured 95% maximum values of background voltage harmonics at the secondary side of the TSS are considered and listed in Table IV.

B. Typical Harmonic Results of the RES

Three scenarios are conducted for investigating the effects of different types of electric trains in terms of their harmonic spectra, i.e., one high-speed train, one thyristor-controlled train, and both. And the typical harmonic spectra of the trains are given in Appendix I.

The resulted harmonic distortions of the three scenarios at T-bus in the TSS are calculated through harmonic power flow process and are compared in Fig. 21. The resonance $f = 16.55$ p.u. significantly increases the distortion of the 17th, 15th, and 19th harmonics. The thyristor-controlled train highly affects the low-frequency harmonics below 20 p.u., while the high-frequency harmonics beyond 40 p.u. are mainly determined by characteristic harmonics of the PWM-controlled train. Due to the higher distortion of the thyristor, the harmonic problem of the thyristor-controlled train is more serious than that of the PWM-controlled train. Comparison results also verify the three harmonic sources presented in Section I. Due to the space limit, typical mitigation schemes and results for RESs will be generally described in the following section.

VII. HARMONIC SUPPRESSION SCHEMES

A. Overview of Harmonic Suppression

For solving the harmonic and resonance problems which are mainly caused by electronic devices and other NLLs, power filters are the dominant solution. There are three basic modes: active, passive, and both treatments. There are three categories of technical methods used to deal with the three harmonic types of harmonic distortions [50], [51].
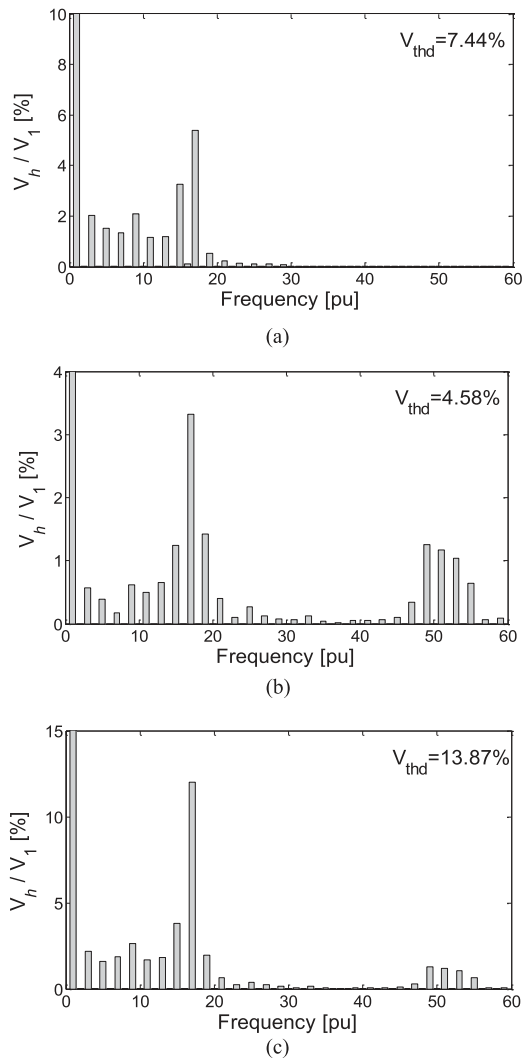
Fig. 21. Harmonic results of three scenario. (a) Thyristor-controlled train, $V_{thd} = 7.44\%$. (b) PWM train, $V_{thd} = 4.58\%$. (c) (a) + (b), $V_{thd} = 13.87\%$.

1) The first category includes the methods that eliminate or reduce the harmonic current emission of the nonlinear devices. Therefore, one can go via optimizing the control strategies of the converter, harmonic compensation controls of the converter, and adjusting grid-tied filter parameter to decrease harmonic emission of the source [52]–[54]. The common purpose of these schemes is to suppress the root of the harmonic source [11]. However, these schemes are not practical in some specific scenarios because of the wide frequency band of various types of the nonlinear devices. Meanwhile, harmonic distortion may be easily amplified by a resonance even though the harmonic emission complies with the standards.

2) Alternatively, harmonic filters (e.g., passive filter, active filter, and hybrid filter) are the common solutions used to reduce the system impedance or compensate antiharmonic currents for voltage distortion suppression [12]. They are applicable to all kinds of harmonic sources. In traditional filtering methods, single-tuned and high-pass filters are widely adopted for mitigating harmonic current injections [12], [14], [40]. Single-tuned filters provide strong atten-

uation at a specific tuned frequency. However, these filters will introduce additional parallel resonance point below the original resonance point. The high-pass filers, such as first order and second order, can be effective for filtering high-frequency components generated by the PWM voltage-source converter (VSC). However, the resistor in series with a capacitor also consumes kilowatts power loss.

3) Besides, we would like to introduce the third scheme. Optimizing/modifying critical or sensitive network parameters to shift the harmful resonance frequencies and offer a lower impedance path at those frequencies [6], [13]. This method can be coordinated with the resonance sensitivity studies, which provide the sensitive indices with respect to each bus, parameter or component.

B. Background Harmonic Suppression

The background voltage harmonics in the RES are caused by the harmonic aggregation of available nonlinear devices connected to the power grid. Therefore, an effective scheme is to filter harmonics in critical down-stream system or secondary side of the transformer that supplies the interest system. As the background harmonics are typically fixed and less fluctuating, passive filters are the better solution, such as the combination of fifth, seventh, and 11st single-tuned filters [55]. The optimizing combination and placement of various filter topologies to achieve a certain harmonic filtering goal in the typical power system are reported in [56].

C. Characteristic Harmonic Suppression

There are two mainstream traction driving modes of electric trains, i.e., thyristor controlled and PWM controlled as aforementioned. The two modes dominate the distribution of characteristic harmonics: 1) the thyristor-controlled train emits rich low-frequency harmonics and does not introduce new harmonic problems; 2) the PWM-controlled train emits higher frequency harmonics that center near intertimes switching frequency.

Dealing with high-frequency characteristic harmonics, two treatments can be applied: 1) optimizing the controls and installing a filter at the onboard 4QC; and 2) filtering the harmonics at TSSs of SPs. Song *et al.* proposed an *LCL* filter for onboard transformer to filter high-frequency characteristic harmonics [32]. Alternatively, some control methods can be used to eliminate selected critical harmonics or shift the centered frequency. The onboard treatment, increasing the mass burden of the train and is not practical. Generally, C-type, second high-order, damped harmonic, and first-order filters are widely used [33].

D. Harmonic Resonance Suppression

The dominant resonances cannot be completely removed but can be shifted. The serious resonance frequency, near the rich harmonic spectrum (e.g., 5 p.u., 7 p.u.), could be shifted to the neighboring frequencies (e.g., 4 p.u., 6 p.u.) where the harmonic current is not sufficient. The harmonic resonance would be therefore weakened. Thus, then, in order to minimize the

cost or adjustment based on the RFS method, the most sensitive parameter or component would be selected. RFS method can be then employed here to eliminate the 17th harmonic problem corresponding to the 16.55 p.u. resonance. Therefore, the resonance 16.55 p.u. can be shifted to either 16 p.u. or 18 p.u. (even harmonics) through the adjustment of the most sensitive component parameters including the equivalent impedance of the traction transformer corresponding to its laps.

On the other hand, in traditional power filters, single-turned and high-pass (e.g., first-order, second-order, third-order, C-type) filters are widely adopted for mitigating harmonic current injections [31], [33], [57], [58]. Based on the present literatures, single-turned and third-order filters will introduce additional parallel resonance point below the original resonance point, although they can provide strong attenuation at a specific tuned frequency. Moreover, some high-pass filters can mitigate high-frequency harmonic effectively, but cannot avoid the kilo-watts power loss produced by the resistor in series with the capacitor.

E. Case Studies

As described above, Scenario 3 in Section VI-B is selected as a test case, with using the following schemes based on 20 Var. The passive filters are placed at the SP according to the bus participation factor results obtained in Fig. 16 [31].

1) Resonance frequency shifting increases the 7.5% tap of the traction transformer. The resonance frequency is shifted to 16.08 p.u. The cost is almost free.
2) Fifth (tuned at 4.8 p.u.), seventh(tuned at 6.8 p.u.), 11th (tuned at 10.5 p.u.) single-tuned filters at SP, total $Q_f = 150$ kVar, the cost is moderate.
3) C-type filter at SP, $Q_f = 150$ kVar, tuned frequency 11 p.u., the cost is moderate.
4) LCL filter in the PWM-controlled train, $L_g = 1.63$ mH, $L_f = 1.3$ mH, $C_f = 125$ μF [22], the cost is huge.
5) 2) + 4).
6) 3) + 4).

Recalling the harmonic power flow procedure, the filtering results of different mitigation schemes are presented in Fig. 22. The following conclusions can be made.

1) Resonance frequency shifting scheme successfully shifts the 16.55 p.u. resonance to 16.08 p.u. and highly reduces the distortions of 17th and 19th harmonics. It is a simple and practical way to mitigate critical resonance issue in normal operations or design stages. As discussed earlier, other parameters can also be selected to achieve the same goal.
2) The passive filter combination of fifth (tuned at 4.8 p.u.), seventh (tuned at 6.8 p.u.), 11th (tuned at 10.5 p.u.) single-tuned filters do not work well since the low-frequency harmonics are not significant. Moreover, these single-tuned filters also bring additional resonances. While, the C-type filter has obtained good filtering results in both resonance and characteristic harmonics.
3) The onboard LCL filter and its combination with the C-type filter are the best selection to suppress almost all

TABLE V
MITIGATION SCHEMES FOR HARMONIC PROBLEMS IN RES

Harmonic parts		Harmonics	Mitigations
Background harmonics		3, 5, 7, 11, 13 p.u.	• Single-tuned filters • Active power filters
Resonance harmonics		15∼30 p.u.	• Frequency shifting • C-type, second order filter, etc. • Active power filters.
Characteristic harmonics	Thyristor-controlled	3∼19 p.u. (odd)	• Single-tuned filters • C-type • Active power filters
	PWM-controlled	45∼50 p.u. (odd)	• High-pass filters • Onboard $LCL/L/LC$ filters • Active power filters

harmonics in the RES. The onboard scheme, cutting the harmonic generation source and blocking the harmonic injections, is an effective filtering scheme. It may increase the weight of train and can be adopted at the design stage.

4) The harmonic standard is important to assess that the mitigation scheme is effective. There are several harmonic (or power quality) standards are applied in the RES, such as International Electro-technical Commission (IEC) IEC-61000-3-6, European Norm (EN51060), IEEE 519, and Chinese National Standard Commission (GB) GB/T 14549 [59]–[62]. According to GB/T 14549, the mitigation schemes shown in Fig. 22 can be assessed, (a), (b), and (c) exceed the 3% limit, and cannot be applied in the RES of China. On the contrary, schemes (d), (e), and (f) are well selected.

F. Summary

On the basis of aforementioned studied and previous works, mitigations for different harmonic problems in the RES are concluded in Table V. These mitigations can also be classified as onboard and ground solutions. The onboard solution owns a perfect filtering performance but with the highest cost. The ground mitigation solutions, either passive or active, are commonly placed in a TSS or an SP.

On the other hand, the ground solution installing power filters at the TSS is also a common way to suppress harmonic problems; combination and parameter selection of available filters is a primary work. In this case, C-type filter gives a good filtering performance in both the resonance harmonics and high-frequency characteristics harmonics.

There will be many better mitigation schemes against the harmonic and resonance problems. Due to the space limit, the comparisons of available filters and mitigation schemes are not fully discussed, one can find these overview papers [50], [63]–[66]. Considering the harmonic behaviors of the RES, some of them can be carefully adopted.

VIII. DISCUSSION AND CONCLUSION

Harmonic resonance problems are inherent in any industrial power systems due to the interaction of inductive and capacitive network parameters. It would be effective to reveal more har-
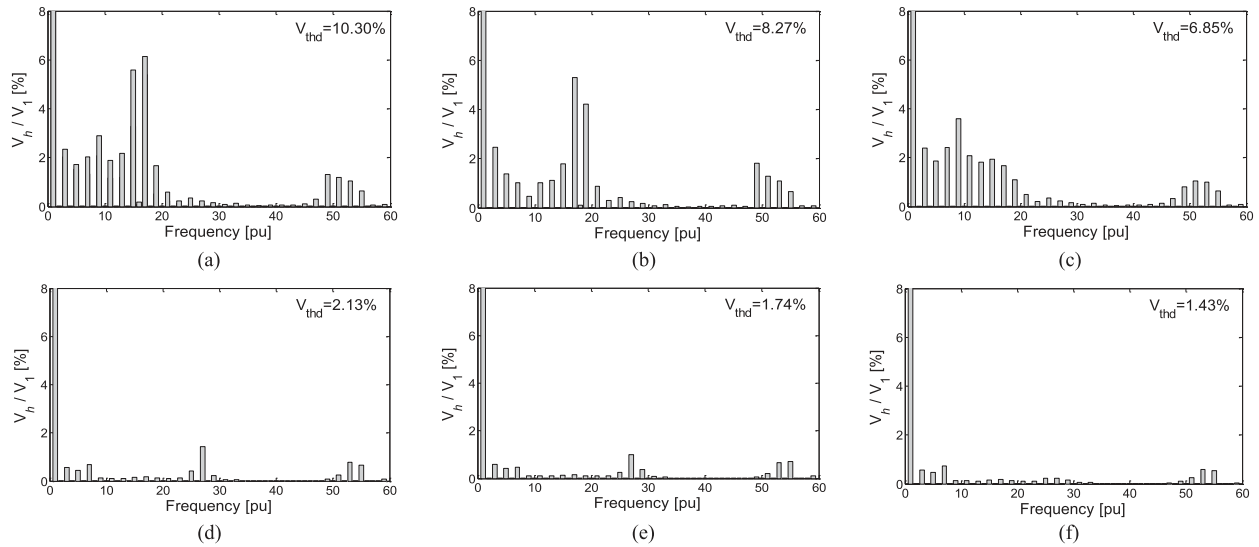
Fig. 22. Filtering results of different mitigation schemes: (a) 1); (b) 2); (c) 3); (d) 4); (e) 2) + 4); and (f) 3) + 4).

monic and resonance information to find solutions to mitigate the harmonic problem in the RES, such as the occurrence mechanism of harmonic and resonance problems, influential factors, effective analysis methods, modeling methods, and suppression schemes. However, there are also some other harmonic problems that needs to be studied in future.

1) How to identify the cause of a serious harmonic distortion in a power system whether it results from a resonance or an aggregated harmonic excitation which is not fully known. It may be identified by comparing the harmonic impedances seen from different buses, especially the adjacent buses, whether they are all at the some resonance point or not. Consequently, the impedance versus frequency curves can be obtained through a specific disturbance injection device. Furthermore, online detection and active control approaches will be necessary to minimize the harmonic effects and power loss of the devices.

2) The classical harmonic current model may be not suitable for the PWM-based 4QC, since the passive harmonic model cannot represent its harmonic behaviors accurately. The output electrical behavior of the 4QC should be taken more attention to address the modeling issue.

3) Resonance instability may oscillate and destabilize the control system of the 4QC if the damping of the control system is not enough [67]. It is different from the harmonic resonance problem. The formation mechanism and associated factors should be taken into attention.

4) As the harmonic spectra and characteristics of different types of electric trains center in different frequency regions, the harmonic and resonance problems may be more complex even in a hub TSS with more railway lines (which increase the resonance points and operate more trains). Therefore, the detailed harmonics in a hub TSS should be considered.

To be concluded, the paper has presented an overview of the harmonic problem in the RES. Harmonic problem sources, analysis methods, modeling methods, influential factors, and suppression schemes were summarized in this paper. Some

TABLE VI
HARMONIC CONTENT OF A THYRISTOR-CONTROLLED TRAIN

h	Content/%	h	Content/%	h	Content/%
1	100	21	0.185	41	0.005
3	15.770	23	0.155	43	0.000
5	10.270	25	0.140	45	0.003
7	5.700	27	0.170	47	0.000
9	4.490	29	0.155	49	0.000
11	1.750	31	0.050	51	0.000
13	0.995	33	0.025	53	0.000
15	0.855	35	0.015	55	0.000
17	0.795	37	0.008	57	0.000
19	0.245	39	0.005	59	0.000

conclusions are obtained that background harmonics, resonance harmonics, and characteristic harmonics are mainly harmonic sources in the RES. Different analysis methods were introduced and compared to perform the resonance results in terms of resonance frequencies. In addition, model of the TPSS based on mathematical model has been applied to better investigate different resonance factors. Furthermore, suppression methods according to different characteristic of harmonic sources in the RES are compared.

APPENDIX I

The harmonic spectrum of a thyristor-controlled train is given in Table VI. The typical harmonic spectrum used in Section III can be found in [31, Table III].

APPENDIX II

The Scott connection traction transformer, which employs two single-phase transformers, is frequently used transformer for transferring three-phase power to two-phase power. The first transformer is called the main transformer, and the second one is called the teaser transformer. Fig. 23 shows the equivalent circuit of the Scott transformer and its α power supply phase.
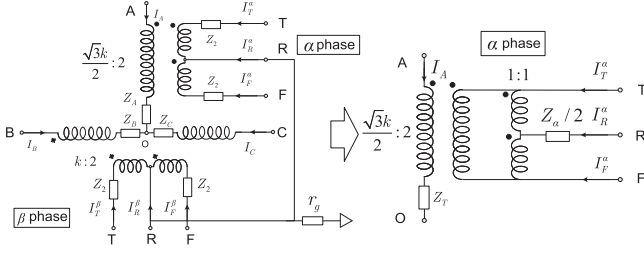
Fig. 23.   Scott traction transformer model.

Fig. 24.   V/v traction transformer model.

As the size and turns ratio of these two transformers are different, their equivalent short-circuit admittance are therefore different. The equivalent short-circuit admittance could be represented by y_M and y_T for the main and teaser transformers, respectively. The node-admittance matrix of the Scott transformer in Fig. 23 and the submatrices in its nodal matrix $\mathbf{Y}_T$ are,

$$\mathbf{Y}_{PP} = \frac{1}{k^2}\begin{bmatrix} \dfrac{4}{3Z_\alpha} & \dfrac{-2}{3Z_\alpha} & \dfrac{-2}{3Z_\alpha} \\[2mm] \dfrac{-2}{3Z_\alpha} & \dfrac{1}{3Z_\alpha}+\dfrac{1}{Z_\beta} & \dfrac{1}{3Z_\alpha}-\dfrac{1}{Z_\beta} \\[2mm] \dfrac{-2}{3Z_\alpha} & \dfrac{1}{3Z_\alpha}-\dfrac{1}{Z_\beta} & \dfrac{1}{3Z_\alpha}+\dfrac{1}{Z_\beta} \end{bmatrix},$$

$$\mathbf{Y}_{PS} = \frac{1}{k}\begin{bmatrix} \dfrac{-2}{\sqrt{3}Z_\alpha} & \dfrac{2}{\sqrt{3}Z_\alpha} & 0 & 0 & 0 \\[2mm] \dfrac{1}{\sqrt{3}Z_\alpha} & \dfrac{-1}{\sqrt{3}Z_\alpha} & 0 & \dfrac{-1}{Z_\beta} & \dfrac{1}{Z_\beta} \\[2mm] \dfrac{1}{\sqrt{3}Z_\alpha} & \dfrac{-1}{\sqrt{3}Z_\alpha} & 0 & \dfrac{1}{Z_\beta} & \dfrac{-1}{Z_\beta} \end{bmatrix}$$

$$\mathbf{Y}_{SS} =$$

$$\begin{bmatrix} \dfrac{1}{kZ_\alpha}+\dfrac{1}{2Z_2} & \dfrac{-1}{kZ_\alpha}+\dfrac{1}{2Z_2} & \dfrac{-1}{Z_2} & 0 & 0 \\[2mm] \dfrac{-1}{kZ_\alpha}+\dfrac{1}{2Z_2} & \dfrac{1}{kZ_\alpha}+\dfrac{1}{2Z_2} & \dfrac{-1}{Z_2} & 0 & 0 \\[2mm] \dfrac{-1}{Z_2} & \dfrac{-1}{Z_2} & \dfrac{4}{Z_2} & \dfrac{-1}{Z_2} & \dfrac{-1}{Z_2} \\[2mm] 0 & 0 & \dfrac{-1}{Z_2} & \dfrac{1}{kZ_\beta}+\dfrac{1}{2Z_2} & \dfrac{-1}{kZ_\beta}+\dfrac{1}{2Z_2} \\[2mm] 0 & 0 & \dfrac{-1}{Z_2} & \dfrac{-1}{kZ_\beta}+\dfrac{1}{2Z_2} & \dfrac{1}{kZ_\beta}+\dfrac{1}{2Z_2} \end{bmatrix}$$

where $Z_\alpha = \frac{4}{3k^2}(Z_A + \frac{Z_X}{4})$, $Z_\beta = \frac{Z_B+Z_C}{k^2}$, $Z_X = 3Z_{BC} - 4Z_A$.

The V/v connection transformer is composed of two single-phase transformers. It steps three-phase power from the primary side, and supplies two single-phase loads on the secondary side. There is phase shifting between two single-phase loads, so an isolation section should be set to isolate two different phases of power. The equivalent circuit model can be made available by the interconnection method, as shown in Fig. 24 [38].
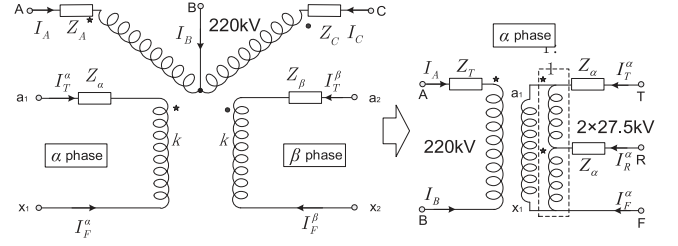
The node-admittance matrix of the V/v transformer can be described by (13) and their vectors are listed as

$$\begin{cases} \mathbf{I}_P = \begin{bmatrix} I_A & I_B & I_C \end{bmatrix}^T, & \mathbf{V}_P = \begin{bmatrix} V_A & V_B & V_C \end{bmatrix}^T \\ \mathbf{I}_S = \begin{bmatrix} I_T^\alpha & I_F^\alpha & I_T^\beta & I_F^\beta \end{bmatrix}^T, & \mathbf{V}_S = \begin{bmatrix} V_T^\alpha & V_F^\alpha & V_T^\beta & V_F^\beta \end{bmatrix}^T \end{cases}. \tag{13}$$

These submatrices in $\mathbf{Y}_T$ can be expressed by

$$\mathbf{Y}_{PP} = \begin{bmatrix} y_T & -y_T & 0 \\ -y_T & 2y_T & -y_T \\ 0 & -y_T & y_T \end{bmatrix},$$

$$\mathbf{Y}_{PS} = \frac{ky_T}{2} * \begin{bmatrix} -1 & 1 & 0 & 0 \\ 1 & -1 & -1 & 1 \\ 0 & 0 & 1 & -1 \end{bmatrix},$$

$$\mathbf{Y}_{SS} = \frac{1}{z_2}\begin{bmatrix} m & n & 0 & 0 \\ n & m & 0 & 0 \\ 0 & 0 & m & n \\ 0 & 0 & n & m \end{bmatrix}$$

in which, y_T, z_1, z_2, m, n, k are similar values as the V/x traction transformer.

For the V/x connection traction transformer, the submatrices in $\mathbf{Y}_T$ are

$$\mathbf{Y}_{PP} = \begin{bmatrix} y_T & -y_T & 0 \\ -y_T & 2y_T & -y_T \\ 0 & -y_T & y_T \end{bmatrix},$$

$$\mathbf{Y}_{PS} = \frac{ky_T}{2} * \begin{bmatrix} -1 & 1 & 0 & 0 & 0 \\ 1 & -1 & 0 & -1 & 1 \\ 0 & 0 & 0 & 1 & -1 \end{bmatrix},$$

$$\mathbf{Y}_{SS} = \frac{1}{z_2}\begin{bmatrix} m & n & -1 & 0 & 0 \\ n & m & -1 & 0 & 0 \\ -1 & -1 & 4 & -1 & -1 \\ 0 & 0 & -1 & m & n \\ 0 & 0 & -1 & n & m \end{bmatrix}$$

in which, $y_T = \frac{1}{Z_T} = \frac{1}{z_1+k^2z_2/2}$, $z_1 = Z_A = Z_C$, $z_2 = 2Z_\alpha$, $n = y_T z_1/2$, $m = (z_1 + k^2z_2)y_T/2$. k is transformation ratio, $k = 220 \text{ kV}/55 \text{ kV}$.

APPENDIX III

TABLE VII
MAJOR PARAMETERS OF POWER SYSTEM, TRACTION
TRANSFORMER AND AT TRANSFORMER

Components	Parameters	Values
V/x transformer	Nominal capacity/MVA	31.5/20/20
	Ratio/kV/kV	$220/2 \times 27.5$
	Impedance voltage	10.5%
	Load loss/kW	143
	No-load loss/kW	31.12
	No-load current	0.14%
AT transformer	Nominal capacity/MVA	16
	Ratio/kV/kV	55/27.5
	Impedance voltage	1.7%
	Load loss/kW	56.412
	No-load loss/kW	11.313
	No-load current	0.071%
Primary lines 2 km	Impedance/Ω/km	$0.0788 + j0.4084$
	Admittance/S/km	1.3509e–6
Secondary lines 0.15 km	Impedance/Ω/km	$0.0470 + j0.0830$
	Admittance/S/km	5.6235e–5

TABLE VIII
CATENARY NETWORK IMPEDANCE AT 50 Hz (x10-1 Ω/KM)

	T_1	F_1	R	T_2	F_2
T_1	$0.802 + 5.905i$	$0.506 + 2.28i$	$0.495 + 3.110i$	$0.489 + 3.336i$	$0.485 + 2.978i$
F_1	$0.506 + 3.228i$	$0.954 + 6.880i$	$0.485 + 3.074i$	$0.485 + 2.978i$	$0.472 + 2.836i$
R	$0.495 + 3.110i$	$0.485 + 3.074i$	$0.568 + 3.633i$	$0.495 + 3.110i$	$0.485 + 3.074i$
T_2	$0.489 + 3.336i$	$0.485 + 2.978i$	$0.495 + 3.110i$	$0.802 + 5.905i$	$0.506 + 3.228i$
F_2	$0.485 + 2.978i$	$0.472 + 2.836i$	$0.485 + 3.074i$	$0.506 + 3.228i$	$0.954 + 6.880i$

TABLE IX
CATENARY NETWORK CAPACITANCE AT 50 Hz (nF/KM)

	T_1	F_1	R	T_2	F_2
T_1	22.59	1.13	3.19	1.86	0.37
F_1	1.13	8.69	3.41	0.37	0.14
R	3.19	3.41	77.31	3.19	3.41
T_2	1.86	0.37	3.19	22.59	1.13
F_2	0.37	0.14	3.41	1.13	8.69

REFERENCES

[1] S. Gao, X. Li, X. Ma, H. Hu, Z. He, and J. Yang, "Measurement-based compartmental modeling of harmonic sources in traction power-supply system," *IEEE Trans. Power Del.*, vol. 32, no. 2, pp. 900–909, Apr. 2017.

[2] Z. He, Z. Zheng, and H. Hu, "Power quality in high-speed railway systems," *Int. J. Rail Transp.*, vol. 4, no. 2, pp. 71–97, Mar. 2016.

[3] H. Lee, C. Lee, G. Jang, and S. Kwon, "Harmonic analysis of the Korean high-speed railway using the eight-port representation model," *IEEE Trans. Power Del.*, vol. 21, no. 2, pp. 979–986, Apr. 2006.

[4] M. Brenna *et al.*, "Investigation of resonance phenomena in high speed railway supply systems: Theoretical and experimental analysis," *Elect. Power Syst. Res.*, vol. 81, pp. 1915–1923, Oct. 2011.

[5] H. Hu, H. Tao, F. Blaabjerg, X. Wang, Z. He, and S. Gao, "Train-network interactions and stability evaluation in high-speed railways–part I: Phenomena and modeling," *IEEE Trans. Power Electron.*, vol. 33, no. 6, pp. 4627–4642, Jun. 2018.

[6] R. Morrison and J. Corcoran, "Specification of an overvoltage damping filter for the national railways of Zimbabwe," *Proc. Inst. Elect. Eng.*, vol. 136, pp. 249–256, Nov. 1989.

[7] Z. Liu, C. Xiang, Y. Wang, Y. Liao, and G. Zhang, "A model-based predictive direct power control for traction line-side converter in high-speed railway," *IEEE Trans. Ind. Appl.*, vol. 53, no. 5, pp. 4934–4943, Sep./Oct. 2017.

[8] G. Chang, H. Lin, and S. Chen, "Modeling characteristics of harmonic currents generated by high-speed railway traction drive converters," *IEEE Trans. Power Del.*, vol. 19, no. 2, pp. 766–773, Apr. 2004.

[9] Z. Ye, L. Edward, K. Yuen, and M. Pong, "Probabilistic characterization of current harmonics of electrical traction power supply system by analytic method," in *Proc. 25th IEEE Ind. Electron. Soc. Annu. Conf.*, Nov./Dec. 1999, vol. 1, pp. 360–366.

[10] Z. Huang, W. Xu, and V. Dinavahi, "A practical harmonic resonance guideline for shunt capacitor applications," *IEEE Trans. Power Del.*, vol. 18, no. 4, pp. 1382–1387, Oct. 2003.

[11] E. Bompard, E. Carpaneto, G. Chicco, P. Ribaldone, and C. Vercellino, "The impact of public lighting on voltage distortion in low voltage distribution systems," *IEEE Trans. Power Del.*, vol. 16, no. 4, pp. 752–757, Oct. 2001.

[12] X. Jiang and A. Gole, "A frequency scanning method for the identification of harmonic instabilities in HVDC systems," *IEEE Trans. Power Del.*, vol. 10, no. 4, pp. 1875–1881, Oct. 1995.

[13] B. Gustavsen, "Study of transformer resonant overvoltages caused by cable-transformer high-frequency interaction," *IEEE Trans. Power Del.*, vol. 25, no. 2, pp. 770–779, Apr. 2010.

[14] S. Papathanassiou and M. Papadopoulos, "Harmonic analysis in a power system with wind generation," *IEEE Trans. Power Del.*, vol. 21, no. 4, pp. 2006–2016, Oct. 2006.

[15] H. Hu, S. Gao, Y. Shao, K. Wang, Z. He, and L. Chen, "Harmonic resonance evaluation for hub traction substation consisting of multiple high-speed railways," *IEEE Trans. Power Del.*, vol. 32, no. 2, pp. 910–920, Apr. 2017.

[16] A. Dolara, M. Gualdoni, and S. Leva, "Impact of high-voltage primary supply lines in the 2×25 kV-50 Hz railway system on the equivalent impedance at pantograph terminals," *IEEE Trans. Power Del.*, vol. 27, no. 1, pp. 164–175, Jan. 2012.

[17] T. Nakajima, H. Suzuki, K. Temma, and I. Iyoda, "High-order harmonic resonance phenomena of a voltage-sourced converter in cable system," *Elect. Eng. Jpn.*, vol. 150, pp. 26–35, Feb. 2005.

[18] E. Currence, J. Plizga, and H. Nelson, "Harmonic resonance at a medium-sized industrial plant," *IEEE Trans. Ind. Appl.*, vol. 31, no. 4, pp. 682–690, Jul./Aug. 1995.

[19] S. Gomes, N. Martins, S. L. Varricchio, and C. Portela, "Modal analysis of electromagnetic transients in AC networks having long transmission lines," *IEEE Trans. Power Del.*, vol. 20, no. 4, pp. 2623–2630, Oct. 2005.

[20] S. Varricchio, Jr., S. Gomes, and R. Rangel, "Three winding transformer S-domain model for modal analysis of electrical networks," *Int. J. Elect. Power Energy Syst.*, vol. 33, pp. 420–429, Mar. 2011.

[21] W. Xu, Z. Huang, Y. Cui, and H. Wang, "Harmonic resonance mode analysis," *IEEE Trans. Power Del.*, vol. 20, no. 2, pp. 1182–1190, Apr. 2005.

[22] H. Hu, Z. He, Y. Zhang, and S. Gao, "Modal frequency sensitivity analysis and application using complex nodal matrix," *IEEE Trans. Power Del.*, vol. 29, no. 2, pp. 969–971, Apr. 2014.

[23] H. Hu, Z. He, X. Li, K. Wang, and S. Gao, "Power-quality impact assessment for high-speed railway associated with high-speed trains using train timetable-part I: Methodology and modeling," *IEEE Trans. Power Del.*, vol. 31, no. 2, pp. 693–703, Apr. 2016.

[24] E. Thunberg and L. Soder, "A norton approach to distribution network modeling for harmonic studies," *IEEE Trans. Power Del.*, vol. 14, no. 1, pp. 272–277, Jan. 1999.

[25] A. Folting, J. Myrzik, T. Wiesner, and L. Jendernalik, "Practical implementation of the coupled norton approach for nonlinear harmonic models," in *Proc. Power Syst. Comput. Conf.*, 2014, pp. 1–7.

[26] H. Roudsari, A. Jalilian, and S. Jamali, "Resonance assessment in electrified railway systems using comprehensive model of train and overhead catenary system," in *Proc. IET Conf. Railway Traction Syst.*, Apr. 2010, pp. 1–5.

[27] M. Wu, C. Roberts, and S. Hillmansen, "Modelling of AC feeding systems of electric railways based on a uniform multi-conductor chain circuit topology," in *Proc. IET Conf. Railway Traction Syst.*, Apr. 2010, pp. 1–5.

[28] J. He, Z. Huang, and Q. Li, "Measurement and study of background harmonic voltages in power systems," *J. China Railway Soc.*, vol. 27, pp. 28–33, 2005.

[29] J. Duan, Z. Qian, and C. Pei, "Harmonic analysis method for input current of traction system applied in high-speed electric multiple unit," in *Proc. Int. Conf. Electron. Optoelectron.*, Jul. 2011, pp. 30–34.

[30] A. Iagar, G. Popa, and I. Sora, "Analysis of electromagnetic pollution produced by line frequency coreless induction furnaces," *WSEAS Trans. Syst.*, vol. 8, pp. 1–11, Jan. 2009.

[31] H. Hu, Z. He, and S. Gao, "Passive filter design for china high-speed railway with considering harmonic resonance and characteristic harmonics," *IEEE Trans. Power Del.*, vol. 30, no. 1, pp. 505–514, Feb. 2015.

[32] W. Song, S. Jiao, and Y. W. Li, J. Wang, and J. Huang, "High-frequency harmonic resonance suppression in high-speed railway through single-phase traction converter w11th LCL filter," *IEEE Trans. Transp. Electrific.*, vol. 2, no. 3, pp. 347–56, Sep. 2016.

[33] D. Rivas, L. Moran, J. Dixon, and J. Espinoza, "Improving passive filter compensation performance with active techniques," *IEEE Trans. Ind. Electron.*, vol. 50, no. 1, pp. 161–170, Feb. 2003.

[34] X. Sun, J. Zeng, and Z. Chen, "Site selection strategy of single-frequency tuned R-APF for background harmonic voltage damping in power systems," *IEEE Trans. Power Electron.*, vol. 28, no. 1, pp. 135–143, Jan. 2013.

[35] K. Song, M. Wu, V. Agelidis, and H. Wang, "Line current harmonics of three-level neutral-point-clamped electric multiple unit rectifiers: Analysis, simulation and testing," *IET Power Electron.*, vol. 7, pp. 1850–1858, Jul. 2014.

[36] *IEEE Recommended Practice for the Design of Reliable Industrial and Commercial Power Systems Analysis*, IEEE Standard 503, 1999.

[37] L. Sainz, M. Caro, and E. Caro, "Analytical study of the series resonance in power systems with the steinmetz circuit," *IEEE Trans. Power Del.*, vol. 24, no. 4, pp. 2090–2098, Oct. 2009.

[38] T. Chen and H. Kuo, "Network modelling of traction substation transformers for studying unbalance effects," *Proc. Inst. Elect. Eng. Gener. Transmiss. Distrib.*, vol. 142, no. 2, pp. 103–108, Mar. 1995.

[39] D. Holmes, "A general analytical method for determining the theoretical harmonic components of carrier based PWM strategies," in *Proc. IEEE Ind. Appl. Conf.*, Oct. 1998, pp. 1207–1214.

[40] Z. He, H. Hu, Y. Zhang, and S. Gao, "Harmonic resonance assessment to traction power-supply system considering train model in china high-speed railway," *IEEE Trans. Power Del.*, vol. 29, no. 4, pp. 1735–1743, Aug. 2014.

[41] J. Shen and N. Butterworth, "Analysis and design of a three-level PWM converter system for railway-traction applications," *IEE Proc. Elect. Power Appl.*, vol. 144, no. 5, pp. 357–371, Sep. 1997.

[42] J. Shen, J. Taufiq, and A. Mansell, "Analytical solution to harmonic characteristics of traction PWM converters," *IEE Proc. Elect. Power Appl.*, vol. 144, no. 2, pp. 158–168, Mar. 1997.

[43] W. Ko and J. Gu, "Impact of shunt active harmonic filter on harmonic current distortion of voltage source inverter-fed drives," *IEEE Trans. Ind. Appl.*, vol. 52, no. 4, pp. 2816–2825, Jul./Aug. 2016.

[44] D. Serrano-Jimenez, L. Abrahamsson, S. Castano-Solis, and J. Sanz-Feito, "Electrical railway power supply systems: Current situation and future trends," *Int. J. Elect. Power Energy Syst.*, vol. 92, pp. 181–192, Nov. 2017.

[45] R. Hill, "Electric railway traction-part 3: Traction power-supplies," *Power Eng. J.*, vol. 8, pp. 275–285, Dec. 1994.

[46] H. Cui *et al.*, "Resonant harmonic elimination pulse width modulation-based high-frequency resonance suppression of high-speed railways," *IET Power Electron.*, vol. 8, pp. 735–742, 2015.

[47] L. Battistelli, M. Pagano, and D. Proto, "2 × 25-kV 50 Hz high-speed traction power system: Short-circuit modeling," *IEEE Trans. Power Del.*, vol. 26, no. 3, pp. 1459–1466, Jul. 2011.

[48] Z. Liu, G. Zhang, and Y. Liao, "Stability research of high-speed railway EMUs and traction network cascade system considering impedance matching," *IEEE Trans. Ind. Appl.*, vol. 52, no. 5, pp. 4315–4326, Sep./Oct. 2016.

[49] M. Brenna, F. Foiadelli, and D. Zaninelli, "Electromagnetic model of high speed railway lines for power quality studies," *IEEE Trans. Power Syst.*, vol. 25, no. 3, pp. 1301–1308, Aug. 2010.

[50] L. Czarnecki, "An overview of methods of harmonic suppression in distribution systems," in *Proc. IEEE PES Summer Meeting*, Jul. 2000, vol. 2, pp. 800–805.

[51] F. Peng, "Harmonic sources and filtering approaches," *IEEE Ind. Appl. Mag.*, vol. 7, no. 4, pp. 18–25, Jul./Aug. 2001.

[52] P. Davari, F. Zare, and F. Blaabjerg, "Pulse pattern-modulated strategy for harmonic current components reduction in three-phase AC-DC converters," *IEEE Trans. Ind. Appl.*, vol. 52, no. 4, pp. 3182–3192, Jul./Aug. 2016.

[53] A. Reznik, M. Simoes, A. Al-Durra, and S. Muyeen, "LCL filter design and performance analysis for grid-interconnected systems," *IEEE Trans. Ind. Appl.*, vol. 50, no. 2, pp. 1225–1232, Mar./Apr. 2014.

[54] S. Giannoutsos and S. Manias, "A systematic power-quality assessment and harmonic filter design methodology for variable-frequency drive application in marine vessels," *IEEE Trans. Ind. Appl.*, vol. 51, no. 2, pp. 1909–1919, Mar./Apr. 2015.

[55] G. Chang, S. Chu, and H. Wang, "A new method of passive harmonic filter planning for controlling voltage distortion in a power system," *IEEE Trans. Power Del.*, vol. 21, no. 1, pp. 305–312, Jan. 2006.

[56] A. Nassif, W. Xu, and W. Freitas, "An investigation on the selection of filter topologies for passive filter applications," *IEEE Trans. Power Del.*, vol. 24, no. 3, pp. 1710–1718, Jul. 2009.

[57] B. Lin and B. Yang, "Current harmonics elimination with a series hybrid active filter," in *Proc. IEEE Int. Symp. Ind. Electron.*, Jun. 2001, pp. 566–570.

[58] T. Demirdelen, M. Inci, K. C. Bayindir, and M. Tumay, "Review of hybrid active power filter topologies and controllers," in *Proc. IEEE 4th Int. Conf. Power Eng. Energy Elect. Drives*, May 2013, pp. 587–592.

[59] "Quality of electric energy supply harmonics in public supply network," *General Administration of Quality Supervision, Inspection and Quarantine of the People's Republic of China*, 1993.

[60] "Electromagnetic compatibility (EMC)-Part 3-6: Limits-assessment of emission limits for the connection of distorting installations to MV, HV and EHV power systems," IEC 61000-3-6, (Ed. 2), 2008.

[61] *IEEE Recommended Practices and Requirements for Harmonic Control in Electrical Power Systems*, IEEE Standard 519, 1992.

[62] *Voltage Characteristics of Electricity Supplied by Public Electricity Networks*, European Standard EN 51060, 2010.

[63] S. Zainal, P. Tan, and A. Jusoh, "Harmonics mitigation using active power filter: A technological review," *Elektrika J. Elect. Eng.*, vol. 8, pp. 17–26, 2006.

[64] T. Sekar and B. Rabi, "A review and study of harmonic mitigation techniques," in *Proc. Int. Conf. Emerg. Trends Elect. Eng. Energy Manage.*, Dec. 2012, pp. 93–97.

[65] L. Kocewiak, S. Chaudhary, and B. Hesselbsk, "Harmonic mitigation methods in large offshore wind power plants," in *Proc. 12th Int. Workshop Large-Scale Integr. Wind Power Power Syst. Transmiss. Netw. Offshore Wind Farms*, 2013, pp. 443–448.

[66] R. Zahira and A. Fathima, "A technical survey on control strategies of active filter for harmonic suppression," *J. Procedia Eng.*, vol. 30, pp. 686–693, Dec. 2012.

[67] L. Harnefors, X. Wang, A. Yepes, and F. Blaabjerg, "Passivity-based stability assessment of grid-connected VSCs-an overview," *IEEE J. Emerg. Sel. Topics Power Electron.*, vol. 4, no. 1, pp. 116–125, Mar. 2016.

Haitao Hu (S'13–M'14) received the B.S. degree from Zhengzhou University, Zhengzhou, China, in 2010, and the Ph.D. degree from Southwest Jiaotong University, Chengdu, China, in 2014, both in electrical engineering.

From 2013 to 2014, he worked as a Visiting Doctoral Scholar with the University of Alberta, Edmonton, Canada. He is currently an Associate Professor with the School of Electrical Engineering, Southwest Jiaotong University. His main research interests include power quality and harmonics of the electric traction system.

Yang Shao received the B.Sc. and M.Sc. degrees in electrical engineering from Southwest Jiaotong University, Chengdu, China, in 2014 and 2017, respectively.

He is currently working with the Hefei Power Supply Company, China Railway Shanghai Group Co., Ltd. His main research interests include power quality and harmonic suppression of the electric traction system.

Li Tang received the B.S. degree in electrical engineering from Southwest Jiaotong University, Emei, China, in 2017. He is working toward the M.Sc. degree in electrical engineering at Southwest Jiaotong University, Chengdu.

His main research interests include power quality and harmonic resonance of traction power supply system.

Zhengyou He (M'10–SM'13) received the B.Sc. and M.Sc. degrees in computational mechanics from Chongqing University, Chongqing, China, in 1992 and 1995, respectively, and the Ph.D. degree from the School of Electrical Engineering, Southwest Jiaotong University, Chengdu, China, in 2001.

He is currently a Professor with the School of Electrical Engineering, Southwest Jiaotong University. His research interests include signal process and information theory applied to electrical power system, and application of wavelet transforms in power system.

Jin Ma (M'06) received the B.S. and M.S. degrees in electrical engineering from Zhejiang University, Hangzhou, China, in 1997 and 2000, respectively, and the Ph.D. degree in electrical engineering from Tsinghua University, Beijing, China, in 2004.

From 2004 to 2013, he had been a Faculty member with the North China Electric Power University, China. He is currently an Associate Professor with the School of Electrical & Information Engineering, the University of Sydney, Sydney, N.S.W, Australia. His major research interests include power system modeling, nonlinear control system, dynamic power system, and power system economics.

Dr. Ma is the member of CIGRE W.G. C4.605 "Modeling and aggregation of loads in flexible power networks" and the corresponding member of CIGRE Joint Workgroup C4-C6/CIRED "Modeling and dynamic performance of inverter based generation in power system transmission and distribution studies." He is a registered Chartered Engineer in U.K. and a Member of IET.

Shibin Gao received B.S., M.S., and Ph.D. degrees in electrical engineering from Southwest Jiaotong University, Chengdu, China, 1986, 1999, and 2006, respectively.

He is currently a Professor with Southwest Jiaotong University. His research interests include protection and control of electric traction system.